An Ion Gating Mechanism of Gastric H,K-ATPase Based on Molecular Dynamics Simulations

Richard J. Law,* Keith Munson,† George Sachs,† and Felice C. Lightstone*
*Chemistry, Materials, Earth, and Life Sciences Directorate, Lawrence Livermore National Laboratory, Livermore, California 94550; and †Laboratory of Membrane Biology, David Geffen School of Medicine, University of California and Veterans Administration Greater Los Angeles Healthcare System, Los Angeles, California 90024

ABSTRACT Gastric H,K-ATPase is an electroneutral transmembrane pump that moves protons from the cytoplasm of the parietal cell into the gastric lumen in exchange for potassium ions. The mechanism of transport against the established electrochemical gradients includes intermediate conformations in which the transferred ions are trapped (occluded) within the membrane domain of the pump. The pump cycle involves switching between the E1 and E2P states. Molecular dynamics simulations on homology models of the E2P and E1 states were performed to investigate the mechanism of K^+ movement in this enzyme. We performed separate E2P simulations with one K^+ in the luminal channel, one K^+ ion in the occlusion site, two K^+ ions in the occlusion site, and targeted molecular dynamics from E2P to E1 with two K^+ ions in the occlusion site. The models were inserted into a lipid bilayer system and were stable over the time course of the simulations, and K^+ ions in the channel moved to a consistent location near the center of the membrane domain, thus defining the occlusion site. The backbone carbonyl oxygen from residues 337 through 342 on the nonhelical turn of M4, as well as side-chain oxygen from E343, E795, and E820, participated in the ion occlusion. A single water molecule was stably bound between the two K^+ ions in the occlusion site, providing an additional ligand and partial shielding the positive charges from one another. Targeted molecular dynamics was used to transform the protein from the E2P to the E1 state (two K^+ ions to the cytoplasm). This simulation identified the separation of the water column in the entry channel as the likely gating mechanism on the luminal side. A hydrated exit channel also formed on the cytoplasmic side of the occlusion site during this simulation. Hence, water molecules became available to hydrate the ions. The movement of the M1M2 transmembrane segments, and the displacement of residues Q159, E160, Q110, and T152 during the conformational change, as well as the motions of E343 and L346, acted as the cytoplasmic-side gate.

INTRODUCTION

Gastric H,K-ATPase (proton pump) is the transmembrane (TM) enzyme responsible for the creation of the low pH environment in the stomach through an active, electroneutral exchange of cytoplasmic protons for luminal K^+ (1). As a member of the P2-type ATPase family, the pump cycle involves switching between the E1 and E2P states, with autophosphorylation from ATP driving the protein into E2P, as protons are pumped into the lumen of the stomach (Fig. 1 *A*). The K^+ then enters the membrane domain from the lumen, the enzyme dephosphorylates, and K^+ is trapped (occluded) in the E2K conformation. Relaxation to E1 produces a K^+ transfer to the cytoplasm as the protein (2). The pump maintains the gastric lumen at pH ~0.8 with a million-fold H^+ gradient and a 10-fold K^+ gradient in the opposite direction. Because Na^+ can be substituted for H^+ at higher pH, it is thought that hydronium, rather than protons, is the H^+ species that is pumped (3).

Inhibition of H,K-ATPase is the main goal in the treatment of acid-related diseases such as gastrointestinal esophageal reflux disease (GERD) and duodenal and gastric ulcers. The most successful therapy to date is the application of proton pump inhibitors (PPIs, i.e., omeprazole, lansoprazole, and pantoprazole) that are acid-activated prodrugs. Although these reagents represent a dramatic therapeutic advance, they are not without side effects, and there is room for improvement in the treatment of acid-related diseases. Hence, a detailed knowledge of the molecular structure and mechanism of inhibition of H,K-ATPase remains an important research aim.

The H,K-ATPase enzyme consists of a catalytic α-subunit that contains the ATP, inhibitor, and ion-binding sites, and a smaller, glycosylated β-subunit that provides structural stability and participates in membrane targeting. The α-subunit has 62% sequence identity with the Na-K-ATPase catalytic subunit and 29% sequence identity with srCa-ATPase, which lacks a β-subunit.

Successful crystallization of srCa-ATPase in several different forms has generally defined the mechanism of ion-pumping in the P2-type ATPases in terms of structural intermediates likely to be reasonably homologous across the enzyme family. Although crystal forms of gastric H,K-ATPase have not been obtained, predictive models of H,K-ATPase can be constructed by the process of homology modeling, in which the crystallized derivatives of the srCa-ATPase provide the necessary peptide backbone templates. In general terms, these proteins show five primary domains (Fig. 1 *B*): the TM domain (10 TM helices), and the cytoplasmic stalk, comprised of the

Submitted December 18, 2007, and accepted for publication May 6, 2008.

Address reprint requests to Felice C. Lightstone, Chemistry, Materials, Earth, and Life Sciences Directorate, Lawrence Livermore National Laboratory, L-372, 7000 East Avenue, Livermore, CA 94550. Tel.: 925-423-8657; Fax: 925-424-4334; E-mail: felice@llnl.gov.

Editor: Peter C. Jordan.

0006-3495/08/09/2739/11 $2.00

doi: 10.1529/biophysj.107.128025

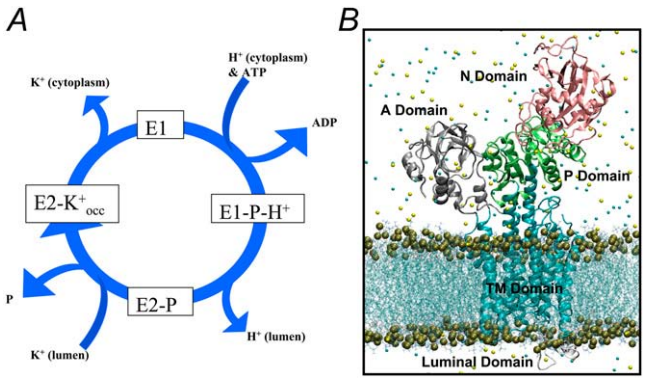

FIGURE 1 (*A*) Catalytic cycle of gastric H,K-ATPase. Protons are transported to the luminal side of the membrane during the ATP-driven transition from the E1 to E2P state, and K^+ activates dephosphorylation to form E2K with occlusion of the ion. Then K^+ is released to the cytoplasm during the conversion back to the E1 state. (*B*) Model of E1 conformation of H,K-ATPase in a lipid bilayer. The protein includes 10 helices in the membrane domain, and three cytoplasmic domains (A, N, and P). The simulation setup is illustrated with the protein hydrated and placed in a POPC bilayer (*gold balls*, POPC phosphate atom), including Na^+ and Cl^- ions (*small cyan* and *yellow balls*). For clarity, water molecules are not shown. Two hydronium ions were added at the ion site near the center of the membrane domain. Either one or two K^+ ions were also added in varying starting positions in each of four separate simulations.

P-domain (where ATP is hydrolyzed), the A-domain, the N-domain, and the exoplasmic domain. The M7-M8 loop contains the site of interaction with the β-subunit, whereas M4 and M5 form helices that extend up into the base of the P domain. The N-, P-, and A-domains undergo large rearrangements during conversion of the E1 to E2P states, and these rearrangements are coupled to changes in the local environment in the ion transport site near the middle of the membrane, which will be investigated in these simulations.

Several key aspects of the mechanism remain unclear. For instance, the ion pathways have not been fully described. Here, we describe the E2P model and an E1 model based on the equivalent E1 form of srCa-ATPase, using molecular dynamics (MD) simulations to further characterize ion movement and trapping in the membrane domain.

In P2-type ATPases, a key requirement is the occlusion of the transported ions during the pump cycle (4). Evidence of this is seen in the E1 structures for srCa-ATPase (5), where the two Ca^{2+} ions are enclosed in the TM domain. A pump cycle can be considered to have two gates that open asynchronously, with the occlusion site in between, so that the ions never gain simultaneous access to both sides of the membrane. In P2 pumps, ATP drives a conformational change that switches ion access and gating of the protein from the inside face to the outside, and must also alter the affinity of the occlusion site for the ions. The molecular details of such a pump mechanism are further complicated by the dynamics of ion dehydration that must play a role in the transport mechanism. As an approach to this problem, a simulation can illustrate possible mechanisms and suggest future experiments to test them (6). In this study, we investigated some important features of K^+ pumping in the H,K-ATPase by using MD simulations to define the occlusion site and identify gating mechanisms.

The available Ca^{2+}-ATPase structures have provided reasonable templates for these conformations (2,7). The E2P state with K^+ occluded can be modeled on the 1WPG E2-MgF (P-analog) Ca^{2+}-ATPase structure (8). This conformation is thought to be homologous to the E2 product state where inorganic phosphate is in the active site, and protons are occluded in the ion site. The structure must undergo relaxation to the E1 state for K^+ to be released, and therefore an exit channel must form during this transition. Although the exact nature of this exit channel is not known, we previously attempted to characterize it (7). The effect of ATP/phosphate binding/release cannot be modeled effectively in terms of its role in this transition, but targeted MD can accurately represent the path of the transition. The E1 state of H,K-ATPase was based on the 1SU4 structure (9), which represents the protein in a state that has Ca^{2+} occluded. It was assumed that conversion to a homologous H,K-ATPase structure allows K^+ to exit, and protons to enter. The motions of the ions and water molecules, and the interactions between the water and the ions, are well within the timescale of MD. Because K^+ is released when E2P transitions to E1, these motions and interactions are the species of interest in understanding the mechanism of K^+ pumping by H,K-ATPase. Therefore, the strategy here is to investigate water, ion, and protein movement with multiple simulations: a simulation in the E2P state with an ion in the luminal channel to explore the lowest energy position for ions in that state, simulations of E2P with one and two K^+ ions in the proposed occlusion site to investigate the coordination of ions at that site, and a targeted MD simulation transitioning the protein from the E2P to the E1 state, and extending the E1 simulation, to investigate cytoplasmic channel formation and possible exit of ions from the occlusion site. Analyzed together, these simulations will provide a description of the path of ions through the complete channel, and the location and nature of the intervening gates.

METHODS

H,K-ATPase homology modeling

Modeling of the H,K-ATPase was described previously (2,7). Both the E2P (pdb.1wpg) (8) and E1 (pdb.1su4) (9) states of the protein were modeled, based on homology with Ca^{2+}-ATPase structures. The alignment was the same as presented previously (2). Detailed descriptions of homology modeling and related sequence identity information are given elsewhere (2). The models are based on the srCa-ATPase crystallized forms, and the N-domain is modeled on the Na,K-ATPase α 2 isoform N-domain, whose sequence is more homologous with H,K-ATPase, but less homologous with srCa-ATPase (10).

Bilayer simulation computational details

In total, four simulations, including protein, water, salt, and a lipid bilayer, were conducted, totaling 61 ns of simulation time in a system comprising

>230,000 atoms. Three 10-ns simulations of the E2P model, i.e., E2P-1K-channel-sim, with one K^+ ion in the luminal channel; E2P-1K-occlusion-sim, with one K^+ ion in the proposed occlusion site; and E2P-2K-occlusion-sim, with two K^+ ions in the proposed occlusion site, and with two hydronium ions (H_3O^+) on the cytoplasmic side of the occlusion site in each case. The initial 110 × 110 Å palmitoyl-2-oleoyl-*sn*-glycerol-phosphatidyl choline (POPC) bilayer slab, with water molecules positioned to hydrate the head groups, was created using the Membrane package in Visual Molecular Dynamics (VMD) (11). This preliminary bilayer, consisting of 326 POPC molecules (163 in each leaflet) and 5529 water molecules, was then relaxed by steepest-descent minimization for 100 steps, and equilibrated in MD for 500 ps, to optimize the lipid-lipid and lipid-water packing.

The H,K-ATPase model was then inserted into the center of the bilayer, and all overlapping lipids and waters were removed. The aromatic girdle residues were lined up with the plane of the membrane. Each system was then fully solvated to a box size of 110 × 110 × 140 Å, using Solvate (12). Enough Na^+ and Cl^- counterions were added to neutralize the charge on the protein and produce a 0.1-M solution. The system was relaxed for 100 steps, followed by a 500-ps equilibration MD run, with the positions of the heavy atoms of the protein restrained to their initial positions throughout. During equilibration, the temperature was raised from 10 K to 310 K, under constant pressure. This restrained run allowed the water and lipid to relax around the protein. Images were prepared, and analysis was performed using HOLE (13) and VMD with tcl/tk scripts.

Targeted MD

The fourth simulation used targeted MD to investigate the conformational transition from the E2P to the E1 state. The simulations included two K^+ ions within the E2P starting structure and still within the E1 targeted structure. The complete system involved 230,000 atoms, and included the protein, POPC lipid bilayer, water, and NaCl counterions. During the enzymatic cycle, K^+ occlusion is associated with phosphate release. The release of phosphate was not modeled here, and the structure of E2P containing bound K^+ that we used at the start of the simulated transition was expected to closely approximate E2K. This structural similarity is observed in srCa-ATPase structures, where pdb.1wpg (homolog of $E_2 \cdot P_i$, the phosphate-release conformation) and pdb.1iwo (the E2 conformation) have a similar root mean-square deviation (RMSD of backbone atoms of 4.3 Å). The ending structure E1K was subsequently examined with extended MD (28 ns) to further investigate the channel water dynamics and a possible K^+ release mechanism (see below).

The E2P to E1 transition was accomplished by applying a small constraining force on the heavy atoms of all residues in the protein, other than those within a 10-Å radius of the potassium starting positions, to target the model to the E1 state. The constraining force takes the form $F = K(r_1 - r_2)^c$ kcal/mol, where K is the set constant for each atom, $r_1 - r_2$ describes the distance between the target and current atom position, and c is the constant exponential to control the distance variable. For a large conformational transition, such as the one examined here, a value of $c = 1$, with variation in K, allows for fine control of the targeting force, and several values of K were tested (data not shown) to obtain the smoothest transition. In the chosen transition, $K = 0.01$ until the RMSD curve began to flatten after 1.2 ns. After this point, the value of K was raised by 0.01 every 100 ps to a final value of 0.18 after 3.1 ns of simulation, with an RMSD from E1 of 1.2 Å. The simulation was continued for a further 28 ns with no force applied, to observe further free motion of the protein, ions, and water.

General molecular dynamics

This report describes a total of 61 ns of MD simulation of four 230,000-atom systems. All MD simulations were run using the CHARMM force field (14) (v27 for lipid and protein) in NAMD (15) with a nonbonded van der Waals cutoff of 9 Å. Parameters for K^+, $H3O^+$, Na^+, and Cl^- are present in the CHARMM force field. The restrained equilibration (500 ps) and production runs were initiated at 10 K and maintained at 310 K by using a Langevin temperature piston. For the constraint force, the value of K used for positional restraints in restrained equilibrium runs was 40 kcal/mol/Å^2 and $c = 2$. Production simulations (those after minimization and equilibration) were conducted at constant pressure. Particle mesh Ewald electrostatics settings were applied to each system. All simulations were run with the SHAKE algorithm (16) and with a 2-fs time step. TIP3P water (17) was used. Molecular dynamics runs were conducted on 512 processors of the MCR machine at the Livermore Computing Center. MCR is a 2304 processor Intel Xeon machine.

RESULTS AND DISCUSSION

Molecular dynamics simulations of the H,K-ATPase α-subunit were used to examine the stability of the homology models, segmental protein mobility, energy wells for K^+ motion in putative E2P state channels, a possible mechanism for the exit of K^+ into the cytoplasm in the E1 state, and the role of water molecules in these mechanisms. Four simulations, including protein, water, salt, and a lipid bilayer, were conducted, totaling 61 ns of simulation time with a system comprising >230,000 atoms. The first three simulations were conducted to monitor ion, water, and protein dynamics in the E2P state. The fourth simulation, with two ions at the now confirmed occlusion site, used targeted MD to drive a conformational change from the E2P to the E1 state of the pump, followed by a longer run on the protein in the E1 state. The results provide insights into the mechanism of K^+ pumping by H,K-ATPase by showing a double-gating mechanism of ion trapping and by helping to define the entry channel, occlusion site, exit channel, and important features of the two gates.

Protein dynamics of the E2P state

The E1 and E2P conformational models of the gastric H,K-ATPase catalytic subunit used in this study were previously presented (2), and are based on the srCa-ATPase crystallized forms, except for the N-domain backbone, with which the Na,K-ATPase α 2 isoform N domain template sequence is homologous to H,K-ATPase but not to srCa-ATPase (10). Such a modification was not employed in other attempts to model either gastric (N. Kim, unpublished data) or colonic H,K-ATPase (18).

The three E2P simulations described here differed in their setup by the number and position of K^+ ions placed within the protein. The E2P-1K-channel-sim simulation had a single K^+ ion placed in the space between M5, M6, M7, and M8 (i.e., the proposed luminal channel), E2P-1K-occlusion-sim had a single K^+ ion in the proposed occlusion site, and E2P-2K-occlusion-sim had two K^+ ions at the occlusion site. The simulations showed the model, in the E2P state, to be stable in the POPC bilayer. The RMSD and root mean-square fluctuation (RMSF) plots help quantify some of the motions seen (Fig. 2, *A* and *B*). The RMSDs (calculated over all

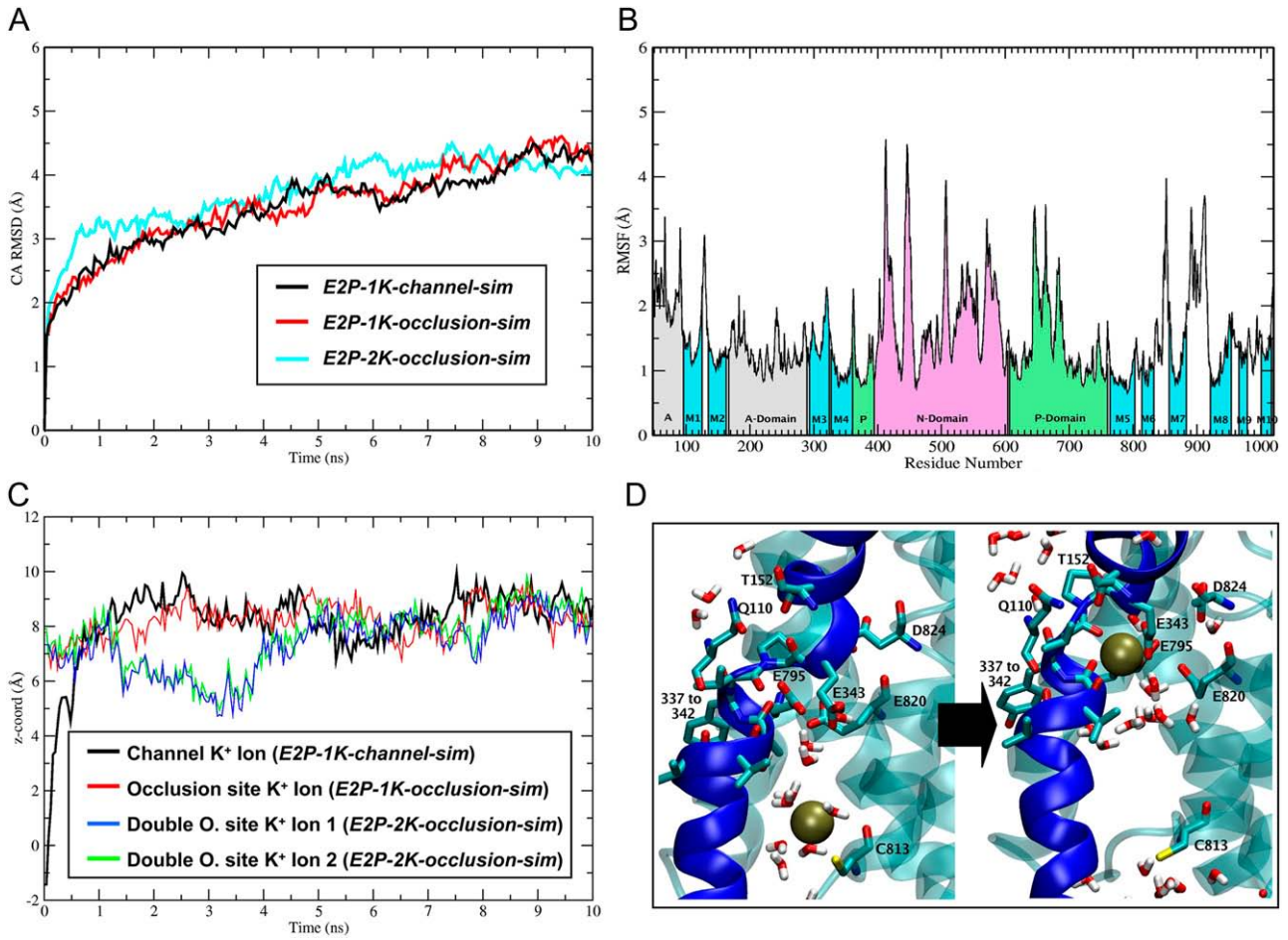

FIGURE 2 Molecular dynamics in three E2P simulations. The simulations differed in the initial position and number of K^+ ions within the membrane domain: E2P-1K-channel-sim started with a single K^+ in the luminal channel, E2P-1K-occlusion-sim with a single K^+ in the occlusion site, and E2P-2K-occlusion-sim with two K^+ ions in the proposed occlusion site. (*A*) The α-carbon dynamics during three simulations, plotted as RMSD versus time. (*B*) Average mobility of various segments of the amino-acid sequence (RMSF), averaged over three simulations. Segments correspond to discrete structural elements, and are color-coded as in Fig. 1 *B*. (*C*) Plot of *z*-coordinate (perpendicular to plane of the membrane) for K^+ ions in the three simulations, normalized for protein motion. The K^+ originating in the occlusion site remains within the site, whereas K^+ in the channel moves into the occlusion site during the E2P-1K-channel-sim simulation. (*D*) Movement of the ion and of associated water molecules. The ion moves from being coordinated by water molecules in the channel around C813 to the occlusion site. The occlusion site is located at the nonhelical section of the M4 transmembrane helix (*dark blue*), where the ion is coordinated by the carbonyl oxygen of residues 337–342, as well as by carboxyl side chains E343, E795, and E820.

α-carbons) as a function of time were very similar for all three E2P simulations, with an average deviation of 2.5–3.0 Å in the first ~1 ns, and approaching a plateau near 4 Å.

The RMSF plot (Fig. 2 *B*) shows which regions of the protein structure contributed to the RMSD values in Fig. 2 *A*. These RMSF values, per α-carbon, were averaged across the three simulations. Relative to the loops and extramembranous domains, the TM segments appear very stable, with <1 Å of fluctuation. The most mobile helices are M1, M2, and M3. Not surprisingly, most of the fluctuations in these structures occur in the cytoplasmic domains, because most of the E2P-to-E1 transition involves these regions. A large amount of motion was seen in the long M7-M8 extracytoplasmic loop. This relatively large loop provides contact with the β-subunit (19,20) that has a structural and possibly regulatory role (21) in pump function. This interaction would be expected to stabilize the loop's conformation. This conclusion and the possible functional significance of intrinsic flexibility in the M7-M8 loop will require testing with a model that includes the β-subunit.

K^+ ion motion in the E2P entry channel and occlusion site

The K^+ ion placed in the luminal channel region of the E2P-1K-channel-sim simulation freely moved up into the putative K^+ binding site (Fig. 2, *C* and *D*), to be coordinated by the backbone carbonyls of the nonhelical section of TM4, i.e., residues 337–342. Although phosphate remains bound at the active site during these simulations, the ligand sphere and protein structure close to the ion site are expected to approximate that of E2K. The inhibitor site for both the PPIs

and the K^+-competitive naphthyridines and [1,2α]-imidazopyridines is near this occlusion site, in the luminal vestibule, and binding would therefore block K^+ access to the occlusion site (2). Experimentally, K^+ remains bound in the E2 state until conversion to E1, during which time the ion exits to the cytoplasmic side. The stability of the final K^+-bound form (Fig. 2 *D*) observed via MD supports this observation. Although the simulations were too brief to see the transition to E1, no such channel, wide enough for a water molecule or K^+ to pass through to the cytoplasmic side of the membrane, can be seen in the E2P model or at any time during the 30 ns of simulation of this state of the protein.

A putative occlusion site, required for the intermediate step in K^+ ion pumping, was previously defined by the position of Ca^{2+} ions in the x-ray srCa-ATPase structures (6,22). The three 10-ns E2P simulations differed mainly in the number of K^+ ions and the position of those ions in the starting configuration. Equilibration allowed water to hydrate the ions appropriately (23), as seen in the nearly octahedral geometry in water molecules coordinating to the K^+ ion in the starting configuration in the E2P-1K-channel-sim simulation (Fig. 2 *D*). Fig. 2 *C* shows the motion of the ions in the three simulations with respect to the *z*-coordinate of the system, which is perpendicular to the plane of the membrane. The single K^+ ion in the luminal channel in the E2P-1K-channel-sim simulation sheds most of its first-shell water molecules (Fig. 2 *D*) and moves into the occlusion site, within the first 2 ns of the simulation, confirming the location and importance of this site in the intermediate binding step in K^+ ion transport. The single-ion position appears to be an average between the positions of the two bound ions in the E2P-2K-occlusion-sim simulation. Whereas a single ion can be completely coordinated by residues at this site, two ions appear to require at least one water molecule to be between the two ions. The ions in the E2P-1K-occlusion-sim and E2P-2K-occlusion-sim simulations, with one and two ions at the occlusion site, respectively, remain in the occlusion site throughout the 10 ns. (No explicit steering or restraining force was applied to any of the ions during the simulation.) After 4 ns, the E2P-1K-channel-sim ion follows the same dynamic profile as the ions in the other two simulations. As in the KcsA K^+-channel structure (24), backbone carbonyls act as surrogate water molecules for the K^+ ions in the occlusion site. The pore loop at the center of the M4 helix provides backbone carbonyls that help coordinate the ion. The occlusion-site carbonyl oxygen atoms come from residues 337–342 on the nonhelical loop at the center of TM helix M4, along with the acidic side chain from E343. Several acidic residues from other TM helices also participate in providing oxygen atoms to coordinate the K^+ ion pair, such as E795 from M5 and E820 from M6. The importance of these negatively charged residues in K^+ ion conduction by the H,K-ATPase channel was previously demonstrated in mutagenesis studies (25–27). The M4 loop alters the conformation slightly to accommodate the incoming ion. The occlusion site is relatively disordered compared with the organization gained by ion binding. Previous work suggested that one of the roles of ion countertransport in this family of pumps is to maintain bound ions at the occlusion site, and to retain the structure of this site for transport of the H_3O^+ ion (28).

In the E2P state, a constriction in the luminal channel occurs halfway between the luminal mouth and the occlusion site caused by V338, on the M4 helix, which protrudes into the otherwise wide, straight channel. In all simulations, V338 is very mobile, and the channel is often wider here than in the starting structure. The importance of this region in the constancy of the luminal channel is illustrated by mutation data for Ca^{2+}-ATPase, showing that an increase in side-chain size for the adjacent A339 causes channel inactivity (29).

It appears from these simulations that the main driving force of the passage of K^+ ions to the occlusion site is the instability of water in the entry channel. Slight breathing motions of the protein, coupled with the entirely hydrophobic lining of the channel (I816, L817, V336, A339, A335, V148, A144, and L141), mean that the column of water and the coordinated ions are only transiently stable in the entry channel, similar to the situation in the aquaporin channel (30,31) and in synthetic hydrophobic channels containing water (32). This formation of a gap in the water column in the luminal channel was seen in all four simulations. The occlusion site therefore represents a lower energy well into which the ions can move. The size and stability of ion-water complexes in the luminal channel may form part of the ion selectivity. As water molecules in the channel evacuate slightly, they leave a hydration gap on the luminal side of the occlusion site, thereby trapping the ions in the occlusion site. A pump must have two gates so that the transported ions never see both sides of the membrane simultaneously. The environment of the entry channel, and the water molecules within it, seem to constitute the luminal side gate for K^+ ion transport. As clearly defined by these three simulations, the water itself, because of the properties of the channel, is trapping the ions at the occlusion site, therefore acting as the luminal side gate. Although the simulation timescale is sufficient to assess the motion of water in the protein environment, it may not have completely explored possible protein conformations that might alter the environment sufficiently to modify this conclusion, or provide an alternate candidate for a luminal gate. Targeted MD enables much more considerable conformational space-searching.

Targeted MD: E2P-to-E1 conformational change

The targeted MD allowed the conformational transition from the E2P to the E1 state (to within 1.2 Å) to occur over the course of 3.1 ns (Fig. 3 *A*). The large conformational change from E2P to E1 ($\sim$12 Å Cα RMSD), associated with the slow step in the cycle (turnover number, $\sim$30/s), would require an extremely long time course, which is not seen in these simulations. The timescale for the conformational transition used

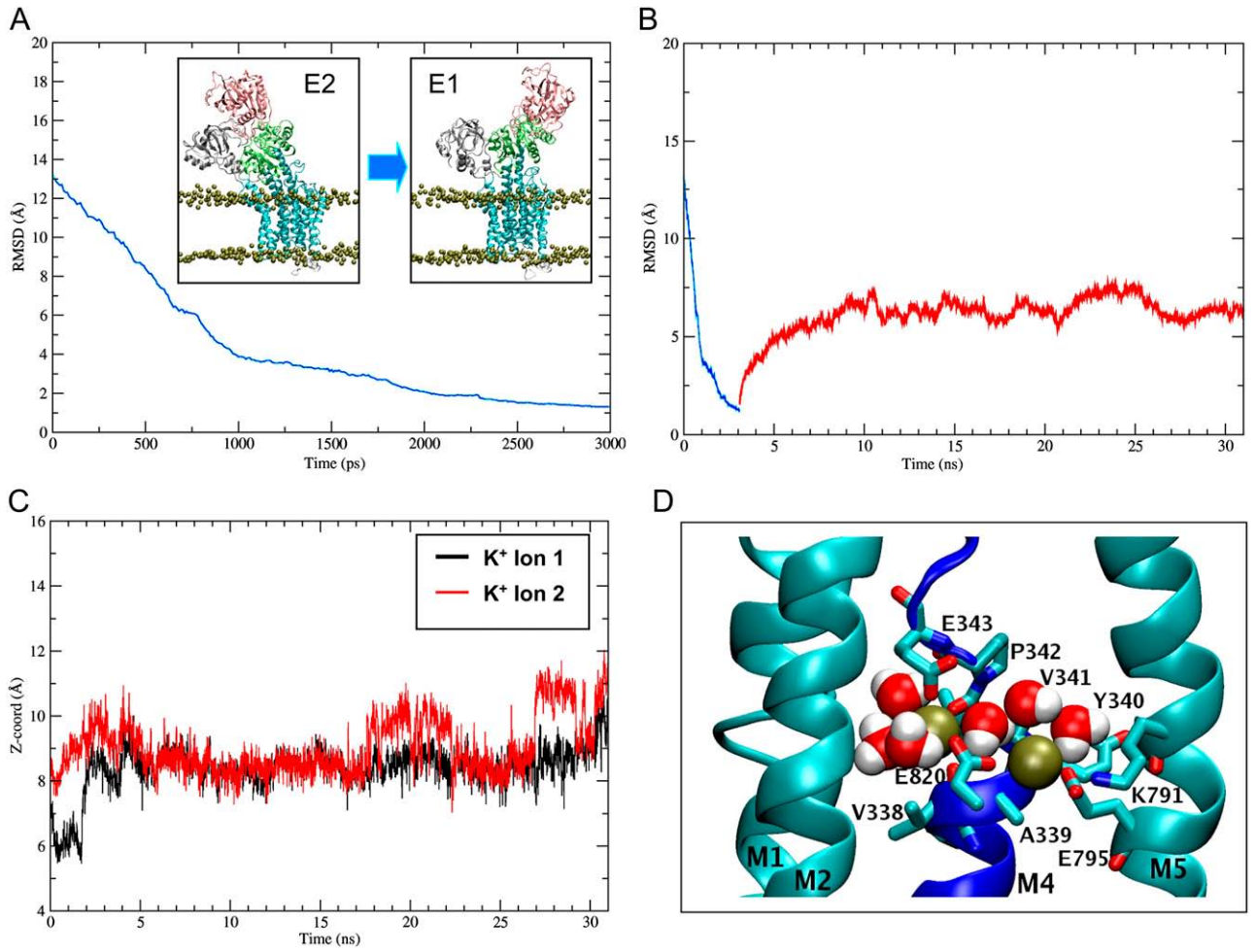

FIGURE 3 Dynamics data for targeted simulation of the E2P-to-E1 transition and for extended dynamics in the E1 state. (*A*) The RSMD over time for targeted MD, as the protein transforms from the E2P conformation to the target E1 state. Once within 1.3Å, after 3.1 ns, the simulation was released to simulate the protein in the E1 state. (*B*) The RMSD for the total 31-ns simulation. (*C*) The *z*-coordinate of the two ions at the occlusion site is plotted. The ions do not leave the occlusion site during the E1 simulation, even though an exit channel to the cytoplasm is formed (Fig. 4 *A*). Small jumps in the position of the ion nearest the exit channel (*red*) represent motions toward the exit as the ion is hydrated by several water molecules that have entered through the exit channel. (*D*) Occlusion-site residues and K^+ ions at the occlusion site at the end of the conversion from the E2P-to-E1 state. The water molecules shown are only those directly associating with K^+ ions. Many more water molecules are present around the exit channel that has now formed in the E1 state (not shown; see Fig. 4 *A*, *right inset*).

here was sufficient to allow movement of the potassium ions and water molecules in and around the protein, should they be disrupted by the transition. The transition from the E2P to E1 state enables water and ion positions to react to the multiple conformational transition states between the start and end states. A 10-Å radius around the proposed occlusion site, including the two K^+ ions placed there, was not directly forced toward any conformation by the targeted MD. The conformation and dynamics in this region were allowed to be influenced only by the transitions taking place elsewhere in the protein. After targeted MD was performed, a simulation of the resulting E1 state was continued for a further 28 ns (Fig. 3 *B*).

The major change in the TM domain occurs in the conformation of M1 and M2 and the relative position of these two helices versus the remainder of the TM domain. As the transition to E1 occurs, both helices straighten considerably and slide ~8 Å down and away from the cytoplasmic domains, toward the luminal side of the membrane. These helices are attached to the A-domain, which undergoes large motions throughout the transition, and they form part of the lining to the luminal (K^+ entry) channel. The luminal entry channel does not narrow during the transition, and the HOLE program analysis still finds a pore on that side of the occlusion site. Hence, the luminal channel appears to be open, in terms of radius, in both the E2P and E1 states (Fig. 4 *A*), but the residues lining the channel near the occlusion site are different because of the shift in the M1 and M2 segments. This shift may play an important role in biasing the water-column instability involved in the gating of the luminal

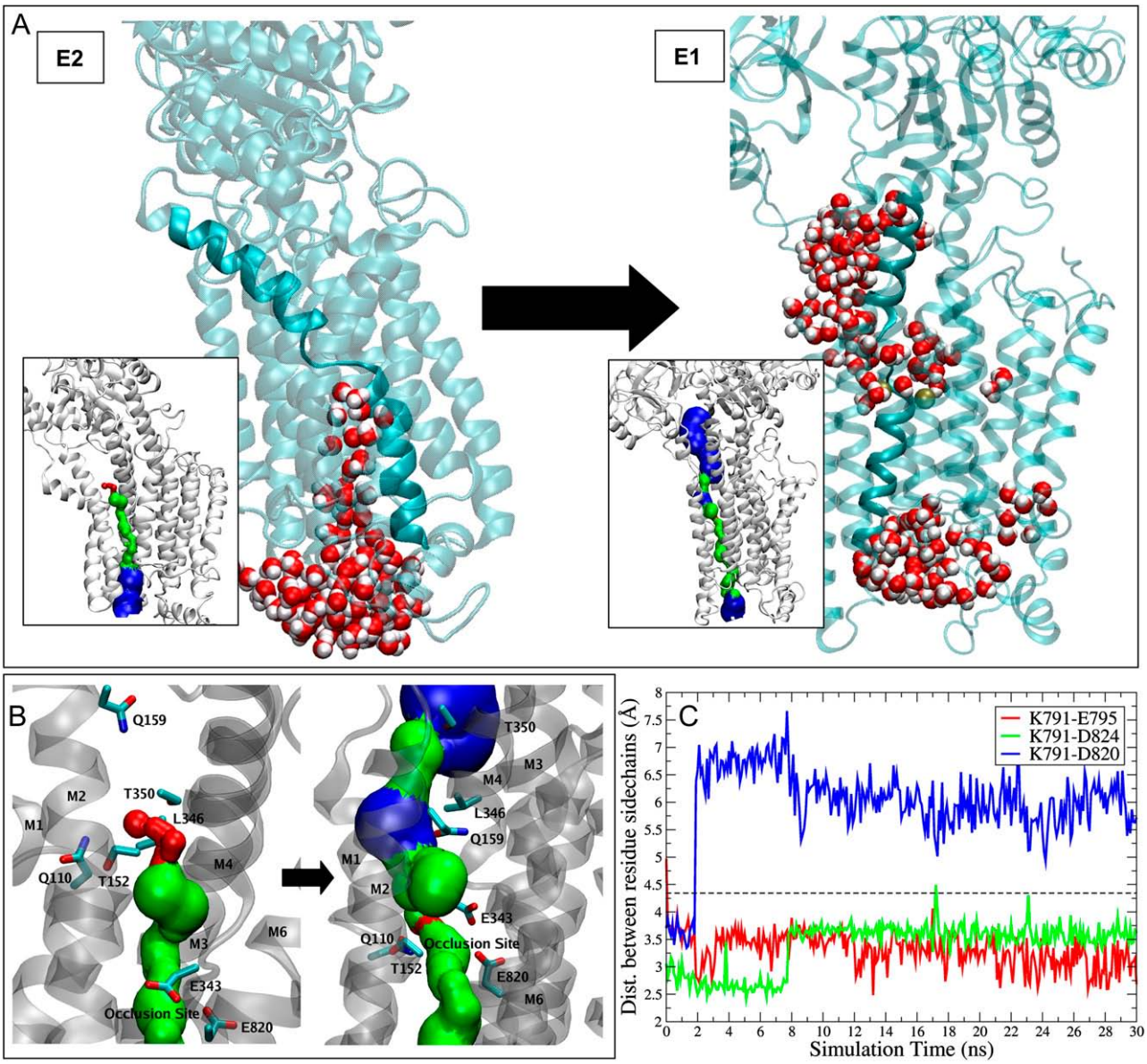

FIGURE 4 (*A*) Protein and water structural changes during transition from the E2P to E1 state. Water in the TM section of the protein is shown in the two different states. During the 31-ns E1 simulation, water penetrates to a position next to the occlusion site, and enters the ligand field of bound K^+. Bulk water and water-hydrating lipid headgroups and the extramembranous part of the protein are not shown, for clarity. A gap in the luminal-channel waters, mainly because of the hydrophobic lining of the channel, appears from these simulations to be an important step in trapping K^+ ions at the occlusion site. Insets: Profiles generated by the HOLE program. (*B*) These profiles, in more detail. In the E2P state, the open entry channel is blocked above the occlusion site by residues L346, T350, T152, and Q110. T152, on the M2 helix, and Q110 are shifted ~10 Å by the movement of the M1-M2 pair during the E2P-to-E1 transition. This opens up the gate above the occlusion site, and places these polar residues proximal to the occlusion site, in a previously hydrophobic area. The residues help sequester water molecules that transiently coordinate with K^+ and may promote ion exit to the bulk cytosol. Charged residues now line the opening to this exit channel, such as E343 and Q159, E160, and E97 (not shown). Green surfaces represent radii between 1.4 Å and 2.8 Å, blue surfaces represent radii >2.8 Å, and red surfaces represent radii <1.4 Å. The pore is dynamic, and these radii are not static in the locations shown. (*C*) Distances between the K791 side chain and three acidic groups around the occlusion site. Displacement of hydronium from the occlusion site by K791 was suggested as the mechanism of low-pKa generation. The K791-E820 salt-link switches off during the E2-to-E1 transition. This switching is fast because these residues are not directly forced during the transition. The distance between K791 and E795 is initially far, and transitions to constantly flickering around the salt-link cutoff distance. K791-D824 was also selected as an interaction, starting as a salt-link that survives the transition from E2-to-E1, but after 8 ns, the link breaks or transitions to a different state.

channel (discussed above). The same breakage in the water channel that provides the luminal gate is observed in this targeted simulation. A lack of full exploration of the conformation may occur even in such a targeted MD simulation, because only a single path for the conformational search was explored by the targeting. In the E2P state, the lining of the luminal pore is composed almost entirely of hydrophobic residues, except at the wide luminal-side mouth, where there

is a single arginine at the base of M4 and an aspartate at the base of M2. This hydrophobicity and the radius of the luminal pore remain largely unchanged as the transition from E2P to E1 occurs, except for a threonine on M2 (T152) and a glutamine on M1 (Q110) which are thrust into the top of the channel, near the occlusion site, because of the 8-Å shift in the position of the M1 and M2 helices. As the simulation progresses in the E1 state, the T152 and Q110 side chains interact with water molecules and hydronium ions, on the cytoplasmic side of the occlusion site, and may have an important role in coordinating the water molecules required to enter the occlusion site to hydrate the occluded K^+ ions. The T152 and Q110 side chains may also have an important role in guiding K^+ ions out of the occlusion site and into the exit channel formed by the transition to E1.

The transition from E2P to E1 changes the position of the K791 side chain (Figs. 3 *D* and 4 *C*) considerably, relative to the occlusion site. It moves away from the bound K^+ ions, to the side of the occlusion site opposite TM4 and E343. Hence, the exit channel to the cytoplasm does not appear to be in the direction of K791, and its side-chain charge would repel positive ions. The movement away from the occlusion site does coincide with a hydronium ion moving closer to the site. Therefore, displacement of K791 may permit hydronium ions to enter the occlusion site in exchange for K^+, and these will be pumped to the lumen in the opposite half of the reaction cycle (E1 to E2P). In Na,K-ATPase, K791 is replaced by a serine, in an otherwise high sequence identity area, and previous mutagenesis studies around this residue highlighted its importance in K^+ transport (33). The displacement of hydronium from the occlusion site by Lys791 was suggested as the mechanism of low pKa generation, and is consistent with the effects of mutating the homologous lysine (Lys800) in toad-bladder H,K-ATPase (34).

The position of the K791 side chain with respect to the distances to carboxylates in the ion site was therefore monitored to identify potential carboxylate binding partners of K791 during the transition from E2P to E1. Fig. 4 *C* shows side-chain center-of-mass distances between K791 and E795, E820, and D824. In the initial E2P state, K791 shows close interactions with all these carboxyls, suggesting that the pKa lowering effect may arise from sharing the side-chain amino group. At the end of ~2 ns, the protein has progressed approximately to the E1 state (Fig. 3), the link to E820 is lost in a rapid step, and interactions with D824 and E795 are maintained. At this point, the K^+ ion pair has become bound within the site (Fig. 3, *inset*).

Continuing E1 state simulation: protein dynamics

The E1 state produced by the targeted MD simulation was continued for a further 28 ns. We analyzed the water and ion motions within the protein, and examined protein dynamics for the model. The Cα-RMSD for this stage of the simulation is depicted as the red line in Fig. 3 *B*. The protein reaches a steady conformation after 7 ns of simulation. The protein does not revert back toward the E2P state (as could be concluded from the plot in Fig. 3 *B*), but simply samples new local conformations around the E1 state. The structural fluctuations in the protein subdomains of the E1 conformation were similar in magnitude to those observed for the averaged E2P simulations (Fig. 2 *B*). As with the E2P state simulations, the most mobile part of the E1 structure was the M7-M8 luminal loop. Its motion in all of the simulations indicates the need for this loop, modeled as a helix to lie on top of the lipid headgroups, in a polar interfacial location. The TM helical sections of M7-M10 are the most stable in the E2P state simulations (Fig. 2 *B*), and the same was seen for the E2P-to-E1 transition and the extended simulation in the E1 conformation. This part of the structure may act as a membrane anchor during conformational changes. Throughout the E1 simulation, water molecules continued to enter the exit channel, and the motions of Q159, E160, E343, and L346 (Fig. 4 *B*) intermittently cut off access of the ions and water at the occlusion site to this exit channel (discussed below).

Potassium ion occlusion in the E1 state

The potassium ion pair does not exit the occlusion site during the full 31-ns simulation, but the K^+ ion closest to the exit channel shows an element of switching into an initial release position in four discrete, short-lived (~2 ns) events during the simulation. This can be seen as discrete moves in the $+z$ direction by the ion closest to the exit channel (Fig. 3 *C*). Analysis shows that these moves are linked to the coordination of this ion by water molecules that entered the protein through the exit channel formed during the transition to the E1 state.

During the conformational transition, little change occurs in the residues involved in the coordination of K^+ at the occlusion site, except in the E343 side chain, which may be an important gating residue. The major change involved the entry of water molecules into the occlusion site as the exit channel formed (Fig. 3 *D*). The ions were coordinated in the E2P state by backbone carbonyls and acidic side chains. During the simulation, water molecules moved to coordinate the ions. For most of the simulation, the ions had a coordination number of six with the surrounding oxygen atoms from the backbone, side chains, and water molecules. Most interestingly, a water molecule inserted itself between the members of the K^+ ion pair (Fig. 3 *D*), to shield their charges from each other, exactly like the K^+ ion transport state in potassium channels (35–37). Formation of the E1 state and the opening of an apparent exit channel bring more water molecules into the occlusion site, to coordinate with the ion nearest the exit channel. By the time the E1 state is reached, four of the six coordinating oxygen atoms on the K^+ nearest the proposed exit channel are from water molecules (Fig. 3 *D*). By having the water molecules exchange with the protein

atoms coordinated to the K^+ ion, the ion decreases its affinity for the occlusion site, and would hypothetically be mobile enough to leave through the newly formed exit channel, with its first solvation shell. This is clearly an important step in the release of ions from the occlusion site to the cytoplasm, and such an affinity-lowering event is vital in the function of such a pump. The water molecules that solvate the K^+ ions in the occlusion site come completely from the side that the ions are being pumped to, suggesting that water is not pumped across the membrane along with the counterion, as previously suggested for the possible mechanism of Ca^{2+}-ATPase (28).

It was previously suggested, although not observed, that incoming hydronium ions may play a role in the displacement of K^+ ions from the occlusion site (6). Although this was not observed in any of the simulations, one of the two hydronium ions in the system did migrate to a position near the occlusion site (as K791 moves away), yet it never succeeded in displacing the K^+ ion during the simulation. It is likely that the timescale of such as event is longer than the length of the simulation.

Exit-channel formation in the E1 state

Fig. 4 *A* shows the pore profiles from the HOLE analysis, as well as some of the water molecules associated with the protein, to demonstrate the presence of water in the entry channel (Fig. 4 *A*, *left inset*). The HOLE analysis was run on 10-ps snapshots throughout the simulation. Initially, the pore is seen to be blocked just above the occlusion site. As the transition from E2P to E1 occurs, a channel opens up, revealing an exit channel up between the M1-M2 slab and M3. Usually (in most snapshots), the exit is seen going past the A-domain (Fig. 4 *A*), but transiently finds a shorter exit out of the top of the TM domain, again between M1-M2 and M3, without going through the gap formed between the A-domain and the rest of the cytoplasmic stalk. This shorter exit path may be blocked by the lipid, however, which was not included in the HOLE calculation. A phospholipid headgroup was assigned to density in the space between M2 and M6 in an E2P homolog of $srCa^{2+}$-ATPase (pdb.2agv) (28). A similar lipid between M1 and M3 may assist in the formation of the exit channel in H,K-ATPase.

Water molecules enter the newly formed exit channel (Fig. 4 *A*, *right inset*). The majority of the transition that allows this channel to form relates to the sliding of the M1-M2 slab, as discussed above. Residues directly involved in what could be described as a gate are seen near the occlusion site, on the cytoplasmic side, as the exit channel forms. The movement of M1-M2, and the related movement of Q110 and T152, have the effect of opening a channel to the cytoplasmic side of the membrane. The channel is closed above the occlusion site (Fig. 4 *B*) in the E2P state by the association of Q110 and T152 with T350 and L346 on the M4 transmembrane helix. The motion of M1-M2 during the transition allows the channel to open as T152 is displaced to the occlusion site and forms an interaction with E343 (Fig. 4 *B*). Sitting at what was previously the constriction point in E2P, T350 interacts with Q159 in what could prove vital in terms of lining a solvated pore with polar side chains, including E160. The polar residues (T350, E343, and Q110) that are now at the occlusion site attract more water into the occlusion area, to help hydrate the K^+ ions that are bound there. The L346 side chain remains mobile throughout the simulation and transiently shuts off the channel, even in the E1 state.

Several residues near the exit channel were mutated, as suggested by the modeling and simulation. Apparently both Q159 and E160 line the exit channel and straddle the pore in which water enters from the cytoplasmic side into the occlusion site (Fig. 4 *B*). A Q159E mutant shows a 90% loss in turnover activity and a threefold increase in NH_4^+ $K_{m,app}$, from 2.4 mM to 6.0 mM. The effect was similar, although slightly lower for a Q159N mutation. The opposite effect was observed with E160Q and E160D mutations, which gave lower than wild-type $K_{m,app}$ values of 0.3 mM and 1.1 mM. It was suggested that the charge and side-chain size of these residues are important in coordinating the entry of water into the pore and the passage of hydrated ions out via the same route. Polar residue Q110 is on the M1-M2 slab that moves into the occlusion site during the transition from E2P to E1 (Fig. 4 *B*). A Q110S mutant (serine is the equivalent residue in NaK-ATPase) showed ~50% wild-type activity and an ~50% reduction in K_m to 0.9 mM. Hence the length and polarity of the side chain in this position may influence K^+ ion exit to the cytoplasm from site II.

Complete K^+ ion path through protein

The full path of the K^+ ion can now be extrapolated from multiple simulations and mutagenesis data (Fig. 5). The channel-ion simulation was begun after the ion had already entered through the mouth of the pore and was coordinated by water molecules near C813 but otherwise surrounded by hydrophobic residues such as I816, L817, V336, A339, A335, and M2 residues V148, A144, and L141. This hydrophobic lining destabilizes the waters in the entrance channel, and allows high ion mobility and rapid transfer to the occlusion site. Several acidic side chains (E824, D820, and E795) coordinate the ion and enable the water molecules to be stripped off as it enters the occlusion site. Along with these acidic side chains, plus E343, most of the occlusion site itself is made up of carbonyl backbone oxygen from residues on the loop section at the center of M4, i.e., residues 337–342. Acidic side chain E343 guards the exit from the occlusion site. A single water molecule inserts itself between the members of the K^+ ion pair in the occlusion site as water enters through the exit channel to solvate the ion. The ion's exit from the occlusion site would be aided by the repositioning of Q110 and T152 during the conformational change, which brings these polar side chains into the space bridging the occlusion site to the exit channel. A305 also lines the pore

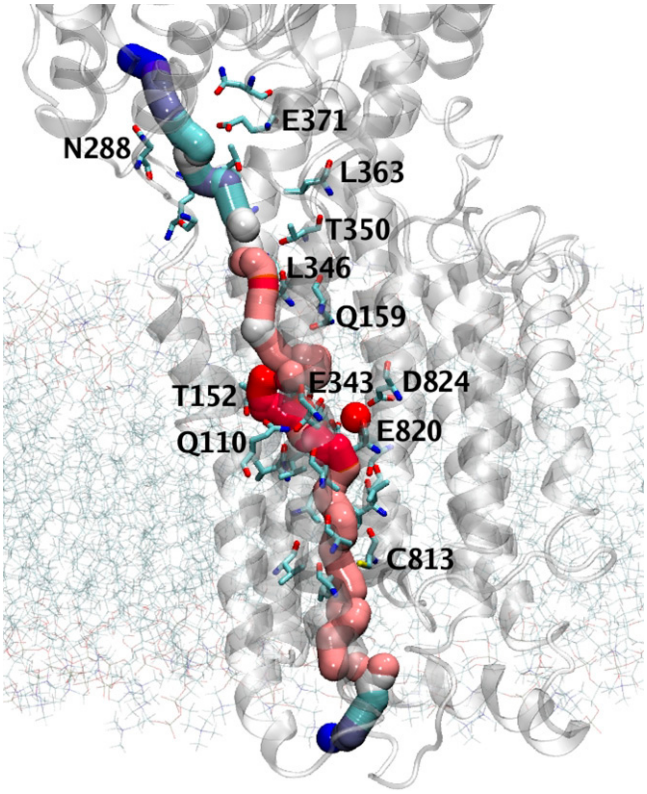

FIGURE 5 Proposed ion path through the protein generated by a combination of simulations, analysis of the protein pores, and water entry in simulation and mutagenesis. The ion path is colored on a red, white, and blue scale. Red-to-pink represents areas of restriction in the pore, including the occlusion site. In white and blue areas, the ion is less restricted by pore geometry, and would likely be hydrated with water molecules because of the hydrophobic nature of the lining of these wider areas of the channel. Some residues involved in the channel are labeled. Protein ribbons were made transparent, and many lipid molecules and ions and all of the water are cut away for clarity.

at this point. The major restriction in the channel above the occlusion site occurs at the position of Q159 and L346. The T350 side chain would help coordinate the ion and water as they move onward toward the mouth of the cytoplasmic exit channel. The channel widens considerably at this point. It is possible that mutations in this region would be more tolerated simply because of the width of the pore. Mostly nonpolar residues (as in the entrance channel) then line the wide exit channel to the mouth, requiring that the ion be hydrated. Residues here include I297, A294, L363, and G94. The mouth itself is defined by polar residues from loops connecting the TM and the cytoplasmic domains, such as K290, T291, N288, E371, and N369.

CONCLUSIONS

These simulations, along with the available mutagenesis data, helped define the mechanism by which K^+ ions are pumped in the H,K-ATPase system. The stability of the model in this POPC bilayer system, in both the E2P and E1 states, indicates that it is amenable to drawing conclusions about its biological function from these studies. Because pumped ions cannot see both sides of the membrane simultaneously, as in an ion-channel protein, an occlusion site must be defined, along with entry and exit gates. Ions entering the luminal channel must be solvated by water because of the hydrophobic lining of the pore, but water is not completely stable in this channel. The lining of the pore and the instability of water in that environment create a gap in the water column that acts as the luminal entry gate. The occlusion site, located at the top of the luminal entry channel, defined by the Ca^{2+} structures and the single-channel ion simulation, represents an energy well as K^+ ions can be stably coordinated to backbone carbonyls of residues in the nonhelical section of TM4 (337, 338, 339, 340, 341, and 342), as well as to the acidic side chains E343, E795, and E820. Simulations show that water molecules play an important role in the coordination of the two K^+ ions at the occlusion site, including an intervening shielding water molecule. Transition from the E2P to E1 state opens a pore to the cytoplasmic side, from the occlusion site. The creation of this pore comes mainly from the motion of the M1-M2 slab as it slides toward the luminal side of the membrane, relative to the rest of the protein. It has the effect of placing two polar residues, Q110 and T152, next to the occlusion site, in the otherwise hydrophobic side-chain environment at the top of the luminal channel. The previous constriction at T350 now opens and is also lined by Q159 and E160, i.e., residues that are conserved in all P2-type ATPase. Coupled with this, the motions of the E343 and L346 side chains together form the exit gate for K^+ ions, as water molecules enter the channel and solvate the ions at the occlusion site. Further mutagenesis investigation of T350 and T152 will help solidify the mechanism of K^+ exit from the protein.

The work of K.M and G.S. is supported by the National Institutes of Health grant DK058333. This work was performed under the auspices of the U.S. Department of Energy by the Lawrence Livermore National Laboratory under contract DE-AC52-07NA27344. The project 06-SI-003 was funded by the Laboratory Directed Research and Development Program at the Lawrence Livermore National Laboratory, UCRL-JRNL-2333318.

REFERENCES

1. Skrabanja, A. T., H. T. van der Hijden, and J. J. De Pont. 1987. Transport ratios of reconstituted ($H^+ + K^+$)-ATPase. *Biochim. Biophys. Acta.* 903:434–440.
2. Munson, K., R. Garcia, and G. Sachs. 2005. Inhibitor and ion binding sites on the gastric H,K-ATPase. *Biochemistry.* 44:5267–5284.
3. Polvani, C., G. Sachs, and R. Blostein. 1989. Sodium ions as substitutes for protons in the gastric H,K-ATPase. *J. Biol. Chem.* 264:17854–17859.
4. Glynn, I. M., and S. J. Karlish. 1990. Occluded cations in active transport. *Annu. Rev. Biochem.* 59:171–205.
5. Toyoshima, C., and H. Nomura. 2002. Structural changes in the calcium pump accompanying the dissociation of calcium. *Nature.* 418:605–611.
6. Sugita, Y., N. Miyashita, M. Ikeguchi, A. Kidera, and C. Toyoshima. 2005. Protonation of the acidic residues in the transmembrane cation-binding sites of the ca(2+) pump. *J. Am. Chem. Soc.* 127:6150–6151.

7. Munson, K., R. J. Law, and G. Sachs. 2007. Analysis of the gastric H,K ATPase for ion pathways and inhibitor binding sites. *Biochemistry*. 46:5398–5417.
8. Toyoshima, C., H. Nomura, and T. Tsuda. 2004. Lumenal gating mechanism revealed in calcium pump crystal structures with phosphate analogues. *Nature*. 432:361–368.
9. Toyoshima, C., M. Nakasako, H. Nomura, and H. Ogawa. 2000. Crystal structure of the calcium pump of sarcoplasmic reticulum at 2.6 Å resolution. *Nature*. 405:647–655.
10. Hakansson, K. O. 2003. The crystallographic structure of Na,K-ATPase N-domain at 2.6 Å resolution. *J. Mol. Biol.* 332:1175–1182.
11. Humphrey, W., A. Dalke, and K. Schulten. 1996. VMD: visual molecular dynamics. *J. Mol. Graph.* 14:33–38.
12. Grubmuller, H., B. Heymann, and P. Tavan. 1996. Ligand binding: molecular mechanics—calculation of the stratavidin-biotin rupture force. *Science*. 271:997–999.
13. Smart, O. S., J. G. Neduvelil, X. Wang, B. A. Wallace, and M. S. P. Sansom. 1996. HOLE: a program for the analysis of the pore dimensions of ion channel structural models. *J. Mol. Graph.* 14:354–360.
14. MacKerrell, A. D., D. Bashford, M. Bellott, R. L. Dunbrack, J. D. Evanseck, M. J. Field, S. Fischer, J. Gao, H. Guo, S. Ha, D. Joseph-McCartney, L. Kuchnir, K. Kuczera, F. T. K. Lau, C. Mattos, S. Michnick, T. Ngo, D. T. Nguyen, B. Prodhom, W. E. Reiher, B. Roux, M. Schlenkrich, J. C. Smith, R. Stote, J. Straub, M. Watanabe, J. Wiorkiewicz-Kuczera, D. Yin, and M. Karplus. 1998. All-atom empirical potential for molecular modeling and dynamics studies of proteins. *J. Phys. Chem. B*. 102:3586–3616.
15. Kalé, L., R. Skeel, M. Bhandarkar, R. Brunner, A. Gursoy, N. Krawetz, J. Phillips, A. Shinozaki, K. Varadarajan, and K. Schulten. 1999. NAMD2: greater scalability for parallel molecular dynamics. *J. Comput. Phys*. 151:283–312.
16. Ryckaert, J. P., G. Ciccotti, and H. J. C. Berendsen. 1977. Numerical integration of the Cartesian equations of motion of a system with constraints: molecular dynamics of *n*-alkanes. *J. Comput. Phys*. 23: 327–341.
17. Sun, Y., and P. A. Kollman. 1995. Hydrophobic solvation of methane and nonbond parameters of the TIP3P water model. *J. Comput. Chem.* 16:1164–1169.
18. Gumz, M. L., D. Duda, R. McKenna, C. S. Wingo, and B. D. Cain. 2003. Molecular modeling of the rabbit colonic (HKalpha2a) H^+, K^+ ATPase. *J. Mol. Model (Online)*. 9:283–289.
19. Colonna, T. E., L. Huynh, and D. M. Fambrough. 1997. Subunit interactions in the Na,K-ATPase explored with the yeast two-hybrid system. *J. Biol. Chem.* 272:12366–12372.
20. Wang, S. G., and R. A. Farley. 1998. Valine 904, tyrosine 898, and cysteine 908 in Na,K-ATPase alpha subunits are important for assembly with beta subunits. *J. Biol. Chem.* 273:29400–29405.
21. Hermsen, H. P., H. G. Swarts, L. Wassink, F. J. Dijk, M. T. Raijmakers, C. H. Klaassen, J. B. Koenderink, M. Maeda, and J. J. De Pont. 2000. The K(+) affinity of gastric H(+),K(+)-ATPase is affected by both lipid composition and the beta-subunit. *Biochim. Biophys. Acta*. 1480:182–190.
22. Toyoshima, C., and G. Inesi. 2004. Structural basis of ion pumping by Ca^{2+}-ATPase of the sarcoplasmic reticulum. *Annu. Rev. Biochem.* 73: 269–292.
23. Ramaniah, L. M., M. Bernasconi, and M. Parrinello. 1999. Ab initio molecular-dynamics simulation of K^+ solvation in water. *J. Chem. Phys.* 111:1587–1591.
24. Doyle, D. A., J. M. Cabral, R. A. Pfuetzner, A. Kuo, J. M. Gulbis, S. L. Cohen, B. T. Cahit, and R. MacKinnon. 1998. The structure of the potassium channel: molecular basis of K^+ conduction and selectivity. *Science*. 280:69–77.
25. Vagin, O., S. Denevich, K. Munson, and G. Sachs. 2002. SCH28080, a K^+-competitive inhibitor of the gastric H,K-ATPase, binds near the M5–6 luminal loop, preventing K^+ access to the ion binding domain. *Biochemistry*. 41:12755–12762.
26. Asano, S., T. Io, T. Kimura, S. Sakamoto, and N. Takeguchi. 2001. Alanine-scanning mutagenesis of the sixth transmembrane segment of gastric H^+,K^+-ATPase alpha-subunit. *J. Biol. Chem.* 276:31265–31273.
27. Swarts, H. G., C. H. Klaassen, M. de Boer, J. A. Fransen, and J. J. De Pont. 1996. Role of negatively charged residues in the fifth and sixth transmembrane domains of the catalytic subunit of gastric H^+,K^+-ATPase. *J. Biol. Chem.* 271:29764–29772.
28. Obara, K., N. Miyashita, C. Xu, I. Toyoshima, Y. Sugita, G. Inesi, and C. Toyoshima. 2005. Structural role of countertransport revealed in Ca(2+) pump crystal structure in the absence of Ca(2+). *Proc. Natl. Acad. Sci. USA*. 102:14489–14496.
29. Clarke, D., T. Loo, W. Rice, J. Anderson, B. Vilsen, and D. MacLennon. 1993. Functional consequences of alterations to hydrophobic amino acids located on the M4 tansmembrane sector of the Ca^{2+}-ATPase of the sarcoplasmic reticulum. *J. Biol. Chem.* 268: 18359–18364.
30. de Groot, B., and H. Grubmuller. 2001. Water permeation across biological membranes: mechanism and dynamics of aquaporin-1 and GlpF. *Science*. 294:2353–2356.
31. Law, R. J., and M. S. Sansom. 2004. Homology modelling and molecular dynamics simulations: comparative studies of human aquaporin-1. *Eur. Biophys. J.* 33:477–489.
32. Hummer, G., J. Rasaiah, and J. Noworyta. 2001. Water conduction through the hydrophobic channel of a carbon nanotube. *Nature*. 414: 188–190.
33. Peluffo, R. D., J. M. Arguello, and J. R. Berlin. 2000. The role of Na,K-ATPase alpha subunit serine 775 and glutamate 779 in determining the extracellular K^+ and membrane potential-dependent properties of the Na,K-pump. *J. Gen. Physiol.* 116:47–59.
34. Burnay, M., G. Crambert, S. Kharoubi-Hess, K. Geering, and J. D. Horisberger. 2003. Electrogenicity of Na,K- and H,K-ATPase activity and presence of a positively charged amino acid in the fifth transmembrane segment. *J. Biol. Chem.* 278:19237–19244.
35. Roux, B., S. Berneche, and W. Im. 2000. Ion channels, permeation and electrostatics: insight into the function of KcsA. *Biochemistry*. 39:13295–13306.
36. Shrivastava, I. H., and M. S. P. S. Sansom. 2000. Simulations of ion permeation through a K channel: molecular dynamics of KcsA in a phospholipid bilayer. *Biophys. J.* 78:557–570.
37. Zhou, Y., J. H. Morais-Cabral, A. Kaufman, and R. MacKinnon. 2001. Chemistry of ion coordination revealed by a K^+-channel-Fab complex at 2.0Å resolution. *Nature*. 414:43–48.